Article

Assessing the Effect of Age and Geomorphic Setting on Organic Carbon Accumulation in High-Latitude Human-Planted Mangroves

Jianxiong Hu [1], **Pei Sun Loh [1,*]**, **Siriporn Pradit [2]**, **Thi Phuong Quynh Le [3]**, **Chantha Oeurng [4]**, **Che Abdul Rahim Mohamed [5]**, **Choon Weng Lee [6]**, **Xixi Lu [7]**, **Gusti Z. Anshari [8]**, **Selvaraj Kandasamy [9]**, **Jianjun Wang [10,11]**, **Zilong Li [1]**, **Haiyan Qin [12]**, **Lili Ji [13]** and **Jian Guo [14]**

[1] Institute of Marine Geology and Resources, Ocean College, Zhejiang University, Zhoushan 316021, China; hjx022498@gmail.com (J.H.); zilongli@zju.edu.cn (Z.L.)

[2] Coastal Oceanography and Climate Change Research Centre, Faculty of Environmental Management, Prince of Songkla University, Hat Yai 90110, Thailand; siriporn.pra@psu.ac.th

[3] Institute of Natural Product Chemistry, Vietnam Academy of Science and Technology, Hanoi 11307, Vietnam; quynhltp@gmail.com

[4] Faculty of Hydrology and Water Resources Engineering, Institute of Technology of Cambodia, Phnom Penh 12156, Cambodia; chantha@itc.edu.kh

[5] Faculty of Science and Technology, Universiti Kebangsaan Malaysia, Bangi 43600, Malaysia; carmohd@ukm.edu.my

[6] Institute of Biological Sciences, University of Malaya, Kuala Lumpur 50603, Malaysia; lee@um.edu.my

[7] Department of Geography, National University of Singapore, 10 Kent Ridge Crescent, Singapore 119260, Singapore; geoluxx@nus.edu.sg

[8] Soil Science Department, Faculty of Agriculture, Tanjungpura University, Pontianak 78124, Indonesia; gzanshari@live.untan.ac.id

[9] Department of Geological Oceanography, Xiang'an Campus of Xiamen University, Xiamen 361102, China; selvaraj@xmu.edu.cn

[10] Jiangsu Key Laboratory of Crop Genetics and Physiology/Jiangsu Key Laboratory of Crop Cultivation and Physiology, Agricultural College of Yangzhou University, Yangzhou 225009, China; wangjianjun@yzu.edu.cn

[11] Jiangsu Co-Innovation Centre for Modern Production Technology of Grain Crops, Yangzhou University, Yangzhou 225009, China

[12] The 11th Geological Section of Zhejiang Province, Wenzhou 325006, China; haiyanqin.geo@gmail.com

[13] Institute of Innovation and Application, Zhejiang Ocean University, Zhoushan 316022, China; jilili@zjou.edu.cn

[14] Zhoushan Sailaite Ocean Technology Co., Ltd., Zhoushan 316100, China; swd60@163.com

* Correspondence: psloh@zju.edu.cn

Abstract: Mangroves are highly productive blue carbon ecosystems that preserve high organic carbon concentrations in soils. In this study, particle size, bulk elemental composition and stable carbon isotope were determined for the sediment cores collected from the landward and seaward sides of two mangrove forests of different ages (M1, ca. 60; M2, ca. 4 years old) to determine the effects of geomorphic setting and age (L1 = old mangrove and S1 = salt marsh stand in M1; L2 = young mangrove and S2 = bare mudflat in M2) on sediments and organic carbon accumulation. The objective of this study was to determine the feasibility of the northernmost human-planted mangroves in China to accumulate sediment and carbon. Our results showed that fine-grained materials were preserved well in the interior part of the mangroves, and the capacity to capture fine-grained materials increased as the forest aged. The biogeochemical properties (C/N: 5.9 to 10.8; δ^{13}C: $-21.60‰$ to $-26.07‰$) indicated that the local organic carbon pool was composed of a mixture of autochthonous and allochthonous sources. Moreover, the accumulation of organic carbon increased with the forest age. The interior part of the old mangrove had the highest organic carbon stock (81.93 Mg C_{org} ha^{-1}). These findings revealed that mangrove reforestation had positive effects on sediments and organic carbon accretion.

Keywords: blue carbon; artificial subtropical mangrove; sediment; carbon sequestration; Ximen Island

1. Introduction

Mangroves occupy tropical and subtropical land–sea margins. They are highly complex ecosystems characterised by high primary productivity, efficient biological nutrient recycling and continuous material exchange with terrestrial and marine ecosystems [1]. Their unique morphological and physiological characteristics (e.g., aerating roots and salt-excreting leaves) favour their survival in waterlogged environments with high salinity and periodic tidal inundation [2]. Because of their high ecological and economic value and their capacity to capture and preserve carbon, mangroves are important blue carbon ecosystems which can help to counter the effects of climate change. These wetland ecosystems are increasingly receiving global attention due to current threats from anthropogenic activities and climatic effects [3,4].

Mangroves are carbon-rich ecosystems that have a more extensive carbon stock (956 Mg C ha^{-1}) than other ecosystems, such as rainforests (241 Mg C ha^{-1}), salt marshes (593 Mg C ha^{-1}) and seagrasses (142.2 Mg C ha^{-1}) [3]. Most organic carbon is stored in the soil and accounts for 77% of the total ecosystem carbon stock [3,5]. Mangroves receive and trap fine sediment materials (i.e., clay and silt) and organic matter from adjacent aquatic habitats (e.g., seagrass meadow) and terrestrial systems via river discharge [6]. Moreover, the friction effect induced by mangrove plants has an active influence on the accumulation of fine-grained materials [7,8]. Their carbon stocks are also markedly influenced by the hydrogeomorphic setting associated with tidal hydrodynamics [9], as tides carry an abundance of sediment into forests and control organic matter decomposition in mangrove soils [9]. Mangrove soils' organic carbon stock varies significantly under different coastal environmental settings. As Twilley et al. [10] reported, mangrove soils' carbon stock is highest in carbonate coastlines, followed by tide/wave-dominated and river-dominated settings. In river-dominated settings, more carbon is allocated to aboveground biomass due to more suitable soil conditions (e.g., low salinity and low water residence time) for plant growth [10]. In carbonate coastlines where river discharge is limited, more carbon is preserved in soil due to enhanced phosphorus foraging by roots [10–12]. In tide/wave-dominated settings, the allocation of carbon between aboveground and belowground biomass is more counterbalanced [10]. There is pronounced variation in carbon stocks even at the mesoscale level (e.g., fringe and interior locations) because of the different hydrodynamic conditions [13]. Interior mangrove locations, with less tidal flushing, are favourable for organic carbon accumulation compared to coastal fringe locations [13,14].

Knowledge of the sources of sedimentary organic carbon is important to better constrain the organic carbon dynamics [15]. Geochemical proxies such as C/N ratios and stable carbon isotope (δ^{13}C) values have been used to indicate the sources of sedimentary organic carbon in coastal areas because they were considered to undergo little change during early diagenesis [16,17]. For example, as the contribution from land-derived organic carbon increases, C/N ratios increase and δ^{13}C values become more depleted. There is a high variability in organic matter sources in mangrove sediments [18], which consist of two primary sources of allochthonous and autochthonous origins [19,20]. Allochthonous organic carbon originates from outside of mangroves, such as marine organic carbon transported through tides and terrestrial organic carbon imported from adjacent river systems. Autochthonous organic carbon results from the in-welling of local mangrove vegetation (e.g., mangrove leaves and branches). Mangrove-derived organic matter often accounts for a lower proportion at seaward fringe locations than landward interior locations [21,22]. Sedimentary organic carbon stocks are not only controlled by hydrogeomorphic settings but are also affected by mangrove species composition, vegetation structure, tree age and climate [23–26]. For example, in restored mangrove forests in Vietnam, as the maturity of the forest increases, the soil organic carbon stocks increase with an increase in the above- and below-ground carbon stocks [27].

Most studies of sedimentary organic carbon stocks and dynamics in Chinese mangroves have been conducted in lower latitude areas of China, including the Hainan [28], Guangxi [29], Guangdong [30] and Fujian [26] provinces. Mangrove forests in Ximen

Island, Zhejiang Province, are currently the northernmost location of mature mangrove ecosystems in China. Since the introduction of the mangrove plant (*Kandelia obovata* Sheue, H.Y.Liu & J.W.H.Yong, 2003) from Fujian Province in 1957, the Ximen Island mangroves have undergone mixed flourishing and deterioration periods. The coverage area of the mangrove forests increased from 0 to 150 ha during the initial 20–30 years and then drastically decreased to 3 ha after some decades because of natural disasters (e.g., extreme cold temperature) and human disturbance (e.g., fishpond construction). Owing to the restoration work that began in 2001, these mangroves currently cover an area of approximately 100 ha on Ximen Island. Studies on mangrove ecosystems in Ximen Island have mainly focused on botany, ecology and the historical development of mangrove based on remote sensing techniques [31,32]. However, to our knowledge, no studies have been conducted on sedimentary organic carbon stocks and dynamics in Ximen Island mangroves. A warm and wet tropical climate is more suitable for mangrove survival. Hence, their survival is threatened by abiotic stress in high latitude, especially from cold temperatures and dry conditions during winter [33]. Mangrove restoration and protection has been given great emphasis in recent years [34], with scientific groups continually trying to expand mangrove areas to higher latitudes [35–37]. Improving the understanding of sedimentary organic carbon stock and dynamics can provide useful insights into the prospects of high-latitude mangrove expansion work. Therefore, in this study, we applied particle size, bulk elemental composition (total organic carbon (TOC) and total nitrogen (TN)) and stable carbon isotope analyses to determine the sources, and the vertical and spatial distribution of sedimentary organic carbon along four sediment cores collected from locations with different geomorphic settings (mangroves, salt marsh stand and bare mudflat) and forest ages (60 and 4 years old). The objective of this study was to determine the ability of human-planted mangrove systems in sub-tropical island climatic zones to accumulate sediment and carbon.

2. Materials and Methods

2.1. Study Area

Calabash-shaped Yueqing Bay is a semi-enclosed sea bay located north of the Ou River estuary in Zhejiang Province and facing the East China Sea (Figure 1a). Spanning approximately 47 km from north to south and 15 km from west to east, Yueqing Bay covers an area of approximately 463.6 km^2 with a coastline of 220 km and a total catchment area of 1470 km^2. More than 30 mountainous rivers discharge into the bay, such as the Dajin and Qing rivers, and all these rivers produce a mean annual runoff of 10.3×10^4 m^3 [31]. The bay is characterised by a northern subtropical oceanic climate. The mean annual temperature is 17–18 °C, and the annual rainfall is 1700 mm [38]. The tides in the bay are irregular and semidiurnal, with average and maximum ranges of 4.2 and 8.34 m, respectively [31,38].

Ximen Island is a special marine-protected area situated at the northern end of Yueqing Bay. Mangrove communities in Ximen Island are a result of human introduction from Fujian Province since 1957. The mangrove ecosystems on Ximen Island represent the northernmost successful artificially cultivated mangrove wetland in China at present. Most of them are found in the upper and middle intertidal zones. *Kandelia obovata* is the only mangrove species here; it has developed well at a high latitude because of its resistance to cold. As a consequence of the introduction of a typical salt marsh vegetation, *Spartina alterniflora*, in 1993, mixed communities comprising mangrove and marsh plants are a characteristic feature of the study area [38,39]. According to the degree of vegetation maturity, they can be classified into two categories: young mangrove communities, which occupy the western part of Ximen Island, where the mangrove trees reach 0.5–0.8 m in height with a vegetation coverage of approximately 20%, and old mangrove communities, which are concentrated on the northeastern side of the island, where the trees have an average height of 2 m and vegetation coverage of approximately 85% [39].
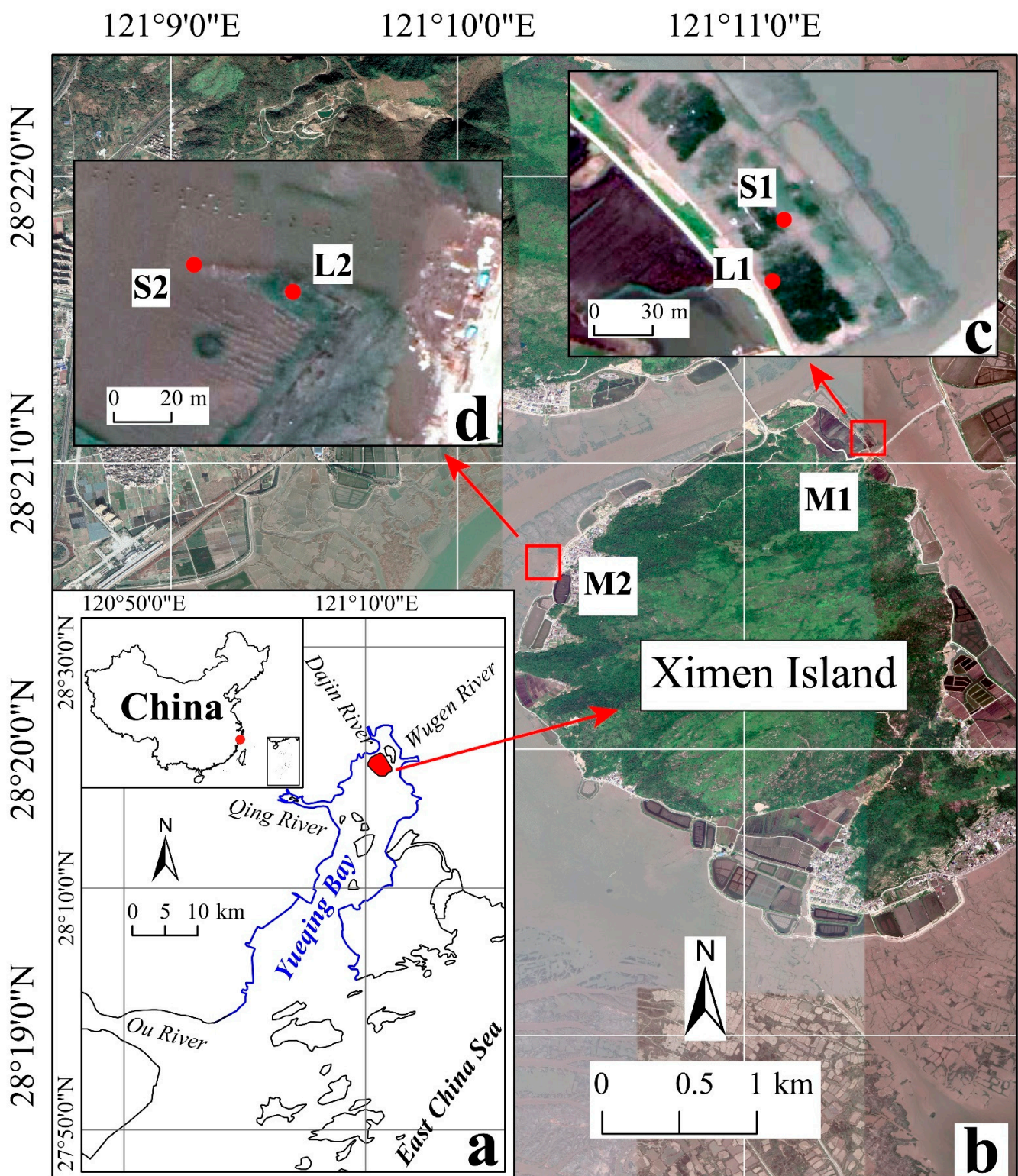
Figure 1. Locations of (**a**) Ximen Island (red area) and Yueqing Bay (blue lined area) in southeastern China; (**b**) two mangrove systems, M1 and M2, on Ximen Island; (**c**) locations of two sediment cores along mangrove M1, L1 and S1; and (**d**) locations of two sediment cores along mangrove M2, L2 and S2.

2.2. Sampling and Samples Pre-Treatment

Sediment cores were collected during low tide on 28 and 29 May 2021 from two mangrove systems, old mangrove (M1) and young mangrove (M2) (Figure 1b), using a gouge auger sampler (1 m (length) × 6 cm (internal diameter)) with minimal compaction.

Mangrove M1 (121°11′25″ E, 28°21′5″ N) is covered by an older mangrove forest with an average age of approximately 60 years and an average height of approximately 2 m, with *Spartina alterniflora* distributed along the fringe of the mangrove forest on the seaward side, thus forming a vegetation transition zone. Sediment cores were collected from two locations in M1: one on the landward side of the older mangrove forest (L1) and the other in the seaward vegetation transition zone which has *Spartina alterniflora* (S1) (Figure 1c). Mangrove M2 (121°10′19″ E, 28°20′38″ N) is dominated by younger mangroves with an average age of approximately four years and an average height of 1.0 m; no other plant species were observed in the area. Along mangrove M2, two sampling locations were selected: one on the landward side covered by the younger mangroves (L2) and the other adjacent to a piece of non-vegetated mudflat on the seaward side (S2; Figure 1d).

Three sediment cores were taken from a triangular plot of approximately 50 cm × 50 cm at each location. Each core was separated into five segments with a 20 cm interval (i.e., 0–20, 20–40, 40–60, 60–80 and 80–100 cm). Each sediment sample was pooled from the same depth from the three cores. All subsamples were stored in plastic bags and kept under 4 °C before further analyses. The mangrove plant (*Kandelia obovata*) and salt marsh plant (*Spartina alterniflora*) tissues were also collected from around the coring sites. The leaves and branches of mangrove trees were separated, and all plant samples were cleaned under running water and oven-dried at 50 °C for 2–3 days; then, they were ground with a grinder to pass through a 50-mesh (355 μm) sieve and stored at room temperature until laboratory analyses [30].

2.3. Sediment and Plant Tissue Analyses

Grain size analyses were conducted using a laser particle size analyser (Mastersizer 2000, Malvern, England), with the measurement size ranging from 0.02 to 2000 μm. Prior to the analyses, the subsamples were treated with 40% H_2O_2 to remove organic matter and 1N HCl to eliminate the inorganic fraction. Each subsample was fractionated into three classes: clay (<4 μm), silt (4 μm–63 μm) and sand (63 μm–2 mm). The Udden–Wentworth grain-size scale was applied as the standard for the objective description of sediment sizes. The moment parameters of grain size distribution, including mean grain size, standard deviation, skewness and kurtosis, were calculated as described in McManus [40] using GRADISTAT for Microsoft Excel (version 9.1, UK) written by Blott and Pye [41].

Prior to the TOC, TN and stable carbon isotope analyses, the ground sediment samples were treated with 1N HCl to remove inorganic carbon. On the following day, the acid was removed and the sediments were oven-dried. Plant samples were determined for the TOC, TN and stable carbon isotope analyses without HCl treatment. TOC and TN contents were measured using an elemental analyser (EA3000, Euro Vector, Italy). The C/N ratio was defined as the TOC/TN molar ratio. Furthermore, stable carbon isotope ratios ($\delta^{13}C$) were measured with an isotope ratio mass spectrometer (Delta Plus, Thermo Fisher Scientific, Waltham, MA, USA), with an average precision of ±0.1‰. The $\delta^{13}C$ values are expressed in per mil units (‰) by using the following equation:

$$\delta^{13}C\ (‰) = (R_{sample}/R_{standard} - 1) \times 10^3, \tag{1}$$

where R = $^{13}C/^{12}C$, R_{sample} is the corresponding ratio of the sample and $R_{standard}$ is the isotope ratio of a standard referenced to Pee Dee Belemnite (PDB).

2.4. Sediment Organic Carbon Stock Calculation

Dry bulk density (DBD) was determined after the mass of the weighted subsamples became constant after oven drying at 105 °C for one week, as follows:

$$DBD\ (g\ cm^{-3}) = Md\ (g)/Vw\ (cm^3), \tag{2}$$

where Md is the mass of the dry samples and Vw is the total volume of the wet samples.

The sediment organic carbon stock of each 2 cm layer (OC_{stock}) was calculated using the following equation:

$$OC_{stock} \ (Mg \ C_{org} \ ha^{-1}) = 100 \times TOC_{layer} \ (g) \div A \ (cm^2), \tag{3}$$

$$TOC_{layer} \ (g) = DBD \ (g \ cm^{-3}) \times H \ (cm) \times A \ (cm^2) \times TOC \ (\%) \times 0.01, \tag{4}$$

where DBD is the dry bulk density; TOC is the total organic carbon content; TOC_{layer} is the mass of organic carbon in each subsample; A is the area of the sample corer and H is the thickness of the sediment (each subsample had a thickness of 2 cm).

To determine OC_{stock} in each 20 cm segment and the whole core, we used the following equation:

$$OC_{stock} \ (Mg \ C_{org} \ ha^{-1}) = DBD_{average} \ (g \ cm^{-3}) \times TOC_{average} \ (\%) \times H' \ (cm), \tag{5}$$

where $DBD_{average}$ and $TOC_{average}$ are the average values of DBD and TOC for all 2 cm subsamples in each 20 cm segment and H' is the thickness of each 20 cm segment.

2.5. Statistical Analyses

Considering that only standard deviation, skewness and dry bulk density passed the normality test (Shapiro−Wilk test), we used the Mann–Whitney U test to compare the differences in the measured parameters among distinct transects and different sampling stations along the same transect. Spearman's correlation analysis was conducted to measure the correlations among the different parameters. A value of $p < 0.05$ was considered significant for the statistical analyses. All statistical analyses were performed using IBM SPSS Statistics for Windows (Version 26.0, IBMCorp, Armonk, NY, USA). All drawings were completed using OriginPro (Version 2021, OriginLab Corporation, Northampton, MA, USA).

3. Results

3.1. Grain Size Analyses

Sediments from all sub-samples showed a singular clay–silt type, which was dominated by the silt (65.75% ± 3.43%) and clay (34.17% ± 3.44%) fractions, followed by a small sand fraction (0.07% ± 0.13%) (Appendix A Table A1). The mean grain size (Mz) ranged from 7.00 φ to 7.63 φ, with an average value of 7.37 φ ± 0.12 φ. The standard deviation (σ) ranged from 1.31 φ to 1.56 φ, with a mean value of 1.44 φ ± 0.04 φ, indicating poor sorting. The skewness (Sk) and kurtosis (Ku) showed mean values of 0.46 ± 0.09 (0.19–0.73) and 2.68 ± 0.14 (2.46–3.16), respectively, suggesting fine-skewed and mesokurtic grain size distribution. All subsamples along each core showed a single peak (Figure 2), and the grain size parameters showed a narrow range, implying a relatively small change in the local sedimentary environment in general.
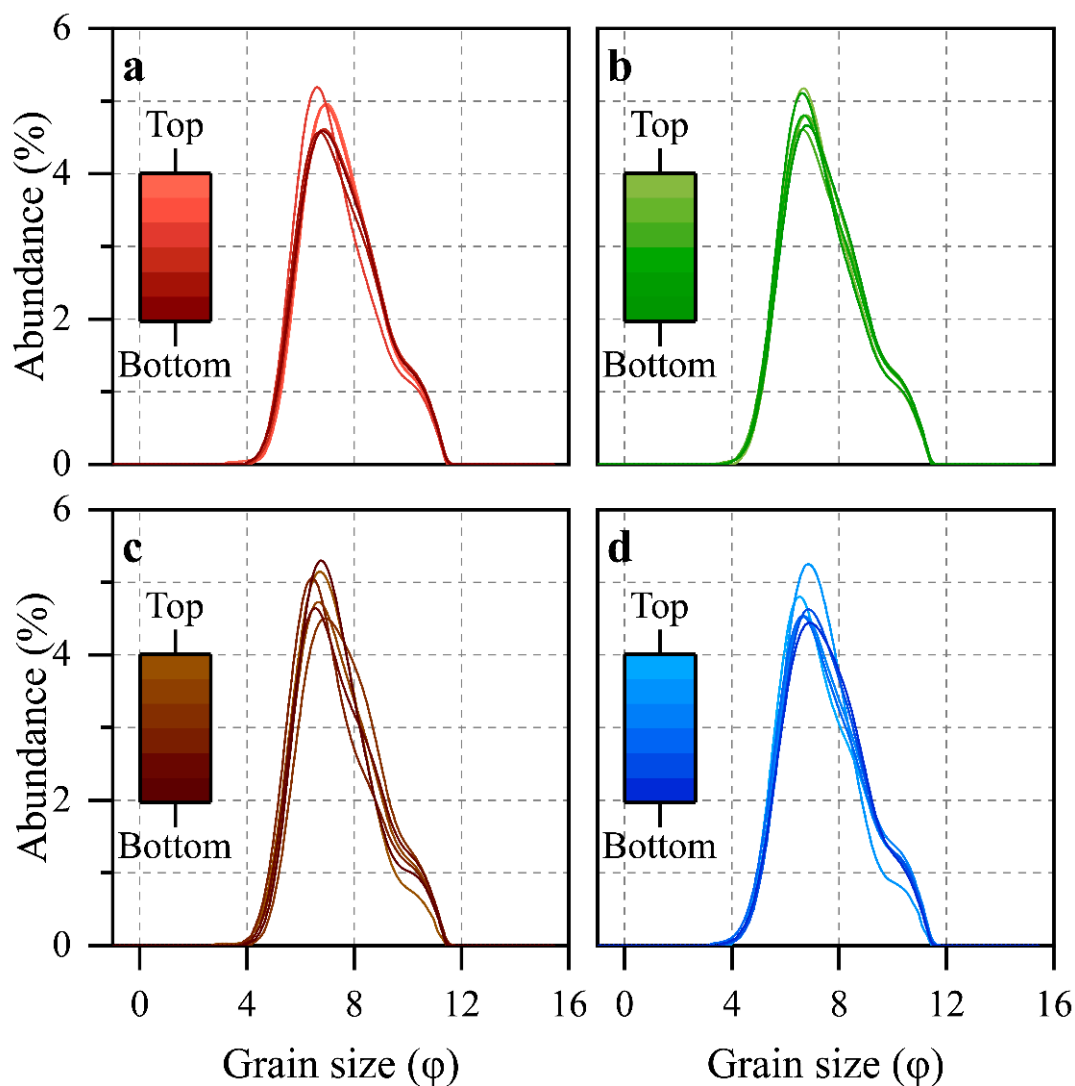
Figure 2. Grain size distribution along sediment cores collected from mangrove M1 at stations (**a**) L1 (old mangrove) and (**b**) S1 (salt marsh stand); and mangrove M2 at stations (**c**) L2 (young mangrove) and (**d**) S2 (bare mudflat). Top and bottom indicate the surface layer and bottom layer of the sediment cores, respectively.

The value of Mz along the surficial sediments of the old mangrove M1 decreased from land (7.51 φ) to seaward (7.32 φ). The value of Sk increased from 0.41 to 0.55 seaward, indicating a coarser fraction on the seaward side; σ and Ku showed no apparent difference between the two sampling stations L1 and S1 (Figure 3). An opposite trend was observed along mangrove M2: the landward area dominated by young mangrove plants (L2) showed a coarser mean grain size of 7.12 φ than the seaward area covered by mudflat (S2) free of vegetation, which had a mean grain size of 7.33 φ. The value of σ increased from land (1.35 φ) to the seaward side (1.50 φ), while that of Ku decreased from 3.00 to 2.55; the value of Sk showed no change.
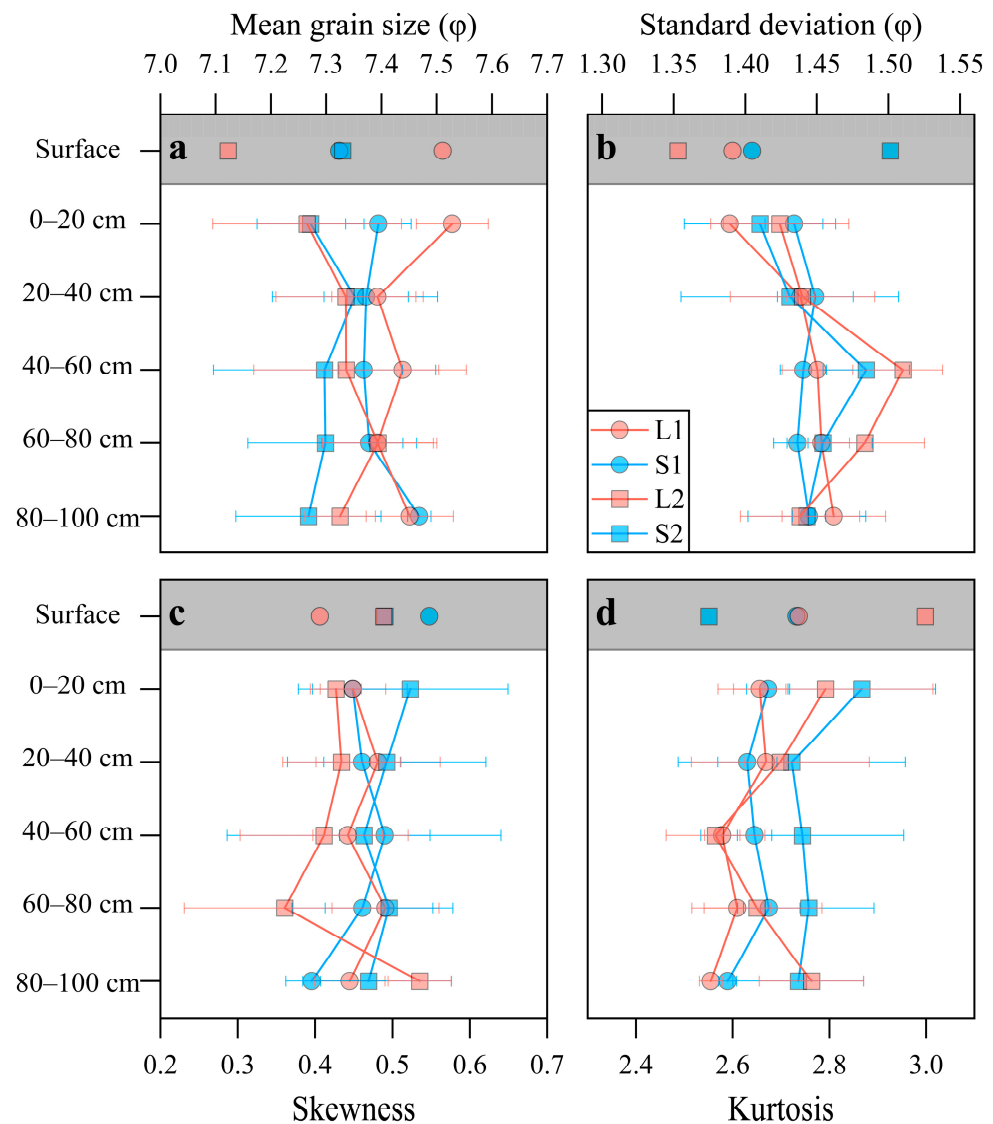
Figure 3. Vertical profile of different parameters (**a**) mean grain size, (**b**) standard deviation, (**c**) skewness and (**d**) kurtosis along the sediment cores. Gray area represents surface sediments at depth of 0–2 cm. Each segment data is presented as mean ± standard deviation. Error bar indicates standard deviation.

Mz at the landward location of mangrove M1 (L1) showed a vertical increasing trend from the bottom to the top layer, while the opposite trend was observed at the landward location of mangrove M2 (L2). No significant variation was observed along the vertical profile at the seaward locations of both mangroves (stations S1 and S2). The value of σ at stations along transect M1 increased from the bottom to the top layers, indicating a weakening of the hydrodynamic environment. At stations along transect M2, σ showed a similar vertical trend of increasing from the 80–100 to 40–60 cm segment and then decreasing to the 0–20 cm segment, indicating a change in the hydrodynamic condition. Sk at station L1 showed no clear variation trend. At stations S1 and S2, Sk increased from the bottom layer to the upper layer, while it decreased from 80–100 cm to 60–80 cm and then increased to the 0–20 cm segment at L2. The value of Ku at station L2 decreased from 80–100 cm to 40–60 cm and then increased to the 0–20 cm segment, while other stations had a general increasing trend from the bottom to the top layer.

3.2. Bulk TOC, TN and $\delta^{13}C$

Results of TOC, TN and $\delta^{13}C$ are given in Appendix A (Table A2). The TOC and TN ranged from 0.56% to 2.04% and 0.094% to 0.220% for all subsamples along the sediment cores. Along the old mangrove M1, the TOC and TN contents of the surface sediments displayed a significant decreasing trend from land (L1) to seaward (S1), but no significant trend was observed along the young mangrove M2 (Figure 4a,b). The vertical profiles along the different cores showed that the TOC content at station L1 increased from 20–40 cm to 0–20 cm, but the increasing trend at S1 and L2 was relatively small, and the TOC content was constant along S2. The TN content showed an increasing trend from the bottom to the top layer at stations L1, S1 and L2, with the trend at station L1 being more significant. The TN content at station S2 decreased from the 80–100 cm to the 40–60 cm segment and then increased to the 0–20 cm segment.
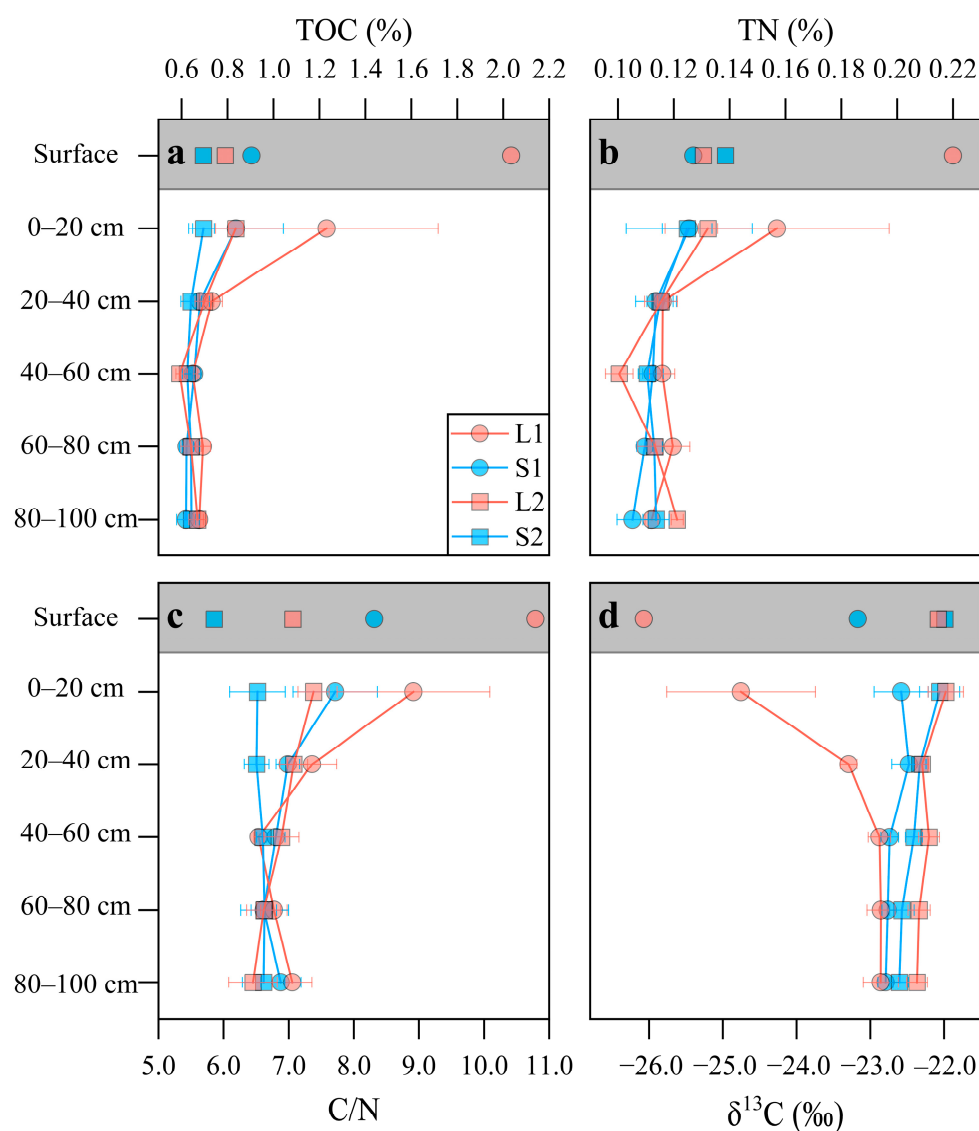
Figure 4. Vertical profile of different parameters (**a**) TOC, (**b**) TN, (**c**) C/N and (**d**) $\delta^{13}C$ along the sediment cores. Gray area represents surface sediments at depth of 0–2 cm. Each segment data point is presented as mean ± standard deviation. Error bar indicates standard deviation.

The C/N value ranged from 5.9 to 10.8 and averaged to 7.0 ± 0.7. The C/N value showed the same distribution pattern along the two mangrove systems, with a higher value on the landward side (Figure 4c). Station L1 had a relatively obvious trend of decreasing

C/N from the 80–100 to the 40–60 cm segment and then increased from the 40–60 cm to the 0–20 cm segment along the core, but the trend along S2 was small. The C/N value increased from the bottom to the top layer at L2, whereas it was constant at station S2. The δ^{13}C value ranged from −21.60‰ to −26.07‰, with a mean value of −22.66‰ ± 0.67‰. δ^{13}C was enriched from land to seaward in the surface sediments along M1, while a small difference was observed along the younger mangrove (Figure 4d). Station L1 had a significant decreasing trend of δ^{13}C values from the bottom to the topmost layer. At the other stations, slightly increasing trends of δ^{13}C values toward the surface layer were observed throughout the vertical profiles.

3.3. Organic Carbon Stocks

The organic carbon stock (OC_{stock}) ranged from 1.08 Mg C_{org} ha^{-1} to 3.43 Mg C_{org} ha^{-1} and averaged to 1.45 Mg C_{org} ha^{-1} ± 0.30 Mg C_{org} ha^{-1} for all subsamples (Appendix A Table A2). In the surface layer, OC_{stock} decreased from land to seaward along M1, but no difference was observed between stations along M2. The vertical profiles of OC_{stock} at stations L1 and S1 increased from the bottom to the upper layer, particularly from the 20–40 cm to the 0–20 cm segment, while no clear variation was observed at stations L2 and S2. The results showed that OC_{stock} along the whole core was the highest at station L1 (81.93 Mg C_{org} ha^{-1}) and the lowest at station L2 (65.53 Mg C_{org} ha^{-1}). The values of OC_{stock} at stations S1 and S2 were 71.72 and 69.52 Mg C_{org} ha^{-1}, respectively. The 0–20 cm segment accounted for a major part of the organic carbon stock at stations S1 (22.6%), L1 (31.9%) and L2 (19.4%), while OC_{stock} at S2 was slightly higher in the bottom than in the upper segment.

4. Discussion

4.1. Sediment Accumulation in Mangroves

Mangroves play a crucial role in regulating sediment transportation and accretion [8,42]. Fine-grained sediments are easily transported by tides as suspended materials are carried landward through tidal pumping [43]; this transport, however, is bidirectional since fine-grained sediments can move back offshore. The friction effect of sediments caused by vegetation (e.g., tree densities and prop roots) has been considered the main factor for the settlement of fine particles in mangrove forests [7,8].

The Mz values were significantly different between mangroves M1 and M2 (*p*-value < 0.05, Mann–Whitney U tests). The higher mean rank at M1 suggested that the particle size at M1 (7.42φ ± 0.09φ) was finer than that at M2 (7.31φ ± 0.13φ). Additionally, along mangrove M1, particle size in surficial sediments increased from land to seaward, while there was an inverse trend along mangrove M2. These results showed that the old mangrove forest (M1) had a more substantial capacity to 'catch hold' of fine-grained sediments than the younger mangrove forest (M2). Old mangrove vegetation can cause a larger reduction in water velocity, thus inducing the deposition of more fine-grained sediments transported into the interior zone. Van Santen et al. [43] showed that current velocity reduced to nearly zero on the mudflat near a mangrove system in the Ba Lat estuary, Vietnam. A study conducted in the Zhangjiang Estuary, Fujian Province, showed that tidal current speed deflected by mangroves had an evident reduction up to 30%−40% [44]. Moreover, in the Tong King delta, Vietnam, Mazda et al. [45] found that the rate of wave reduction in a well-established mangrove area was 6.67–20 times higher than the area with young and sparse vegetation.

Vegetation can create flow obstacles, such as induced complex currents, including jets, eddies and stagnation regions [7,8]. Large flocs consisting of clay and fine silt formed in suspended sediments during tidal inundation remained in suspension because of the turbulence, and then settled during the slack high tide in the forest. Owing to the current sluggishness during ebb tides, the sediments cannot be re-entrained. In addition, the stagnation zones can enhance the trapping effect when the suspended sediments are transported into the forest during spring tide. With stronger friction, old mangroves can trap more fine-grained sediments. Additionally, the Mz value increased from the bottom to

the top layers at the landward site (L1) of mangrove M1, suggesting the potential ability to promote siltation and land-building as the capability to capture fine-grained sediments became stronger as the mangroves aged. Zhu et al. [46] also found that the sediment grain size in the Gaoqiao mangrove, Zhanjiang, Guangdong Province, became finer from the bottom to the upper layers.

Our results showed that unlike Mz and Ku, σ and Sk were limited in their ability to distinguish the sedimentary environment between the two mangrove systems because of the insignificant difference (p-value > 0.05; Mann–Whitney U tests). Ku measured sorting at the tail portion relative to the central portion of the grain size distribution. Excessively well-sorted sediments often have a leptokurtic grain size distribution, while a platykurtic distribution occurs in poorly sorted sediments [47]. Ku presented a significant negative correlation with σ (Spearman's r = −0.452, p < 0.001) in all sediment subsamples, suggesting that Ku can be substituted for σ, which serves as a proxy to indicate the energy condition of the deposition agent. A lower mean rank of Ku at M1 where Ku had a mean value of 2.63 ± 0.06 than that at M2 where Ku had a mean value of 2.73 ± 0.18 indicated a lower energy sedimentary environment in transect M1. This showed that the older mangrove system was more favourable for the deposition of fine-grained particles than the younger mangrove system. This conclusion was supported by the sedimentation rate measurement in Bedono Village, Demak, as Sihombing et al. [48] reported that lowest mangrove density area (600 trees/ha) had the highest sedimentation rate of 30.935 mg/cm^2/day, while the lowest sedimentation rate of 4.891 mg/cm^2/day was found at the highest density area (3100 trees/ha). Van Santen et al. [43] also stated that the densely vegetated area was more sustainable to deposition as it is a more stable area with fewer erosive events.

4.2. Sources and Decay of Sedimentary Organic Matter

The C/N ratio and δ^{13}C value have been widely used in the wetland ecosystem to trace the sources of sedimentary organic carbon (e.g., ref. [49]). As lignin and cellulose are the dominant components in terrestrial plant tissues, terrestrial plants generally have a high C/N value (>12) relative to aquatic plants, bacteria and algae, which typically have lower C/N values (<10) [50]. Because of the different carbon dioxide fixation pathways, C_3 plants commonly showed more depleted δ^{13}C (−21‰ to −32‰) than C_4 plants (−9‰ to −17‰) and marine algae (−16‰ to −23‰) [50]. As the only mangrove species on Ximen Island, fresh *Kandelia obovata* tissues showed a high C/N value (24.2 for leaves and 40.8 for branches) and depleted δ^{13}C (−28.16‰ for leaves and −27.76‰ for branches), within the range typical of C_3 plants. The fresh *Spartina alterniflora* tissues within the mangrove community had a high C/N value of 27.1 and enriched δ^{13}C of −14.74‰ for leaves, as the C_4 plants. The measured C/N and δ^{13}C values of fresh tissues were similar with results from previous studies (Table 1). The C/N and δ^{13}C values of the sediments across the two mangroves, M1 and M2, showed significant differences (p-value < 0.05; Mann–Whitney U tests). The mean C/N value along mangrove M1 (7.2 ± 0.9) was higher than the mean C/N along M2 (6.7 ± 0.4), while the δ^{13}C value at M1 (−23.02‰ ± 0.75‰) was lower than that at M2 (−22.30‰ ± 0.25‰). This indicates that there was more contribution originating from autochthonous materials derived from mangrove plants in the sedimentary organic carbon pool within M1. The older mangrove forest with thicker trunks and denser canopies posed a barrier to prevent autochthonous matter from out-welling; this can explain the significant difference in the two transects.

Table 1. TOC, TN, C/N and δ^{13}C of plant tissues.

	TOC	TN	C/N	δ^{13}C	Reference
	%	%		‰	
Kandelia obovata					
Fresh leaf	39.27	1.896	24.2	−28.16	This study
	41.9–47.2	1.26–1.99			[51]
				−28.1 ± 0.7	[31]
Fresh branch (with bark)	39.50	1.129	40.8	−27.76	This study
Fresh branch bark	45.6–48.6	0.564–0.842			[51]
Fresh branch wood	46.2–47.8	0.347–0.914			[51]
Spartina alterniflora					
Fresh leaf	37.43	1.614	27.1	−14.74	This study
				−15.5 ± 0.4	[31]
	32.69–37.19	1.128–1.679	27.07–29.07		[52]

Partial data for comparison were adapted from ref. [31,51,52].

Compared to the C/N value, the δ^{13}C value was considerably more appropriate and precise for tracing the organic matter source in our study. The C/N value of 10.8 in surficial sediments of the landward site (L1) of mangrove M1 was much lower than that of the fresh tissues of *Kandelia obovata*. This low C/N value can be induced by the preferential loss of carbon over nitrogen from little leaves during early diageneses because of leaching or mineralisation when the exogenetic material inputs were excluded [53,54]. The loss of carbon was up to 95% relative to fresh leaves, whereas the loss of nitrogen was up to 88% in surficial sediments at station L1, which is similar to the findings of Muzuka and Shunula [55]. Moreover, the intercept on the TN axis on the plot of TOC versus TN (Figure 5) was approximately 0.056%, implying the presence of inorganic nitrogen, further suggesting that mineralisation played an important role. However, the measured δ^{13}C value was −26.07‰ in surficial sediments at station L1, which was close to the δ^{13}C value in the fresh tissues of *Kandelia obovata*. The δ^{13}C value exhibited approximately 2‰ enrichment in decomposing mangrove leaves over time [54]. This indicates that the organic matter in surficial sediments underwent a high diagenetic stage before being incorporated into the sediment matrix when the other sources of organic matter were not considered. The relatively stable vertical trends of the C/N and δ^{13}C values were observed in the mudflat core (station S2), indicating the limited influence of microbial activities on organic matter after burial. Therefore, the characteristics of sedimentary organic matter are largely dependent on its nature before incorporation into the sediment texture. If we ignore the contribution of other sources, and only consider the decomposition of mangrove-derived organic matter, the C/N value in the surface sediments at station L1 will show a larger difference relative to the mangrove plant tissues than the δ^{13}C value, which was also observed in the study conducted by Fourqurean and Schrlau [54]. When we only consider the effects of the mixed sources without considering the effect of decomposition, directly using the C/N value has potential issues in quantifying contributions from different sources. For example, using the C/N value of fresh mangrove tissues as an end-member value to quantify the mangrove-derived organic carbon would significantly underestimate the portion derived from mangroves. Hence, the C/N value should be carefully used when applied for quantification, relative to the δ^{13}C value, which shows only a small shift during decomposition. Kennedy et al. [56] also stated that the δ^{13}C value could provide more rigorous source information because of the similar δ^{13}C values obtained from setting particles and sediments contrary to the C/N value.
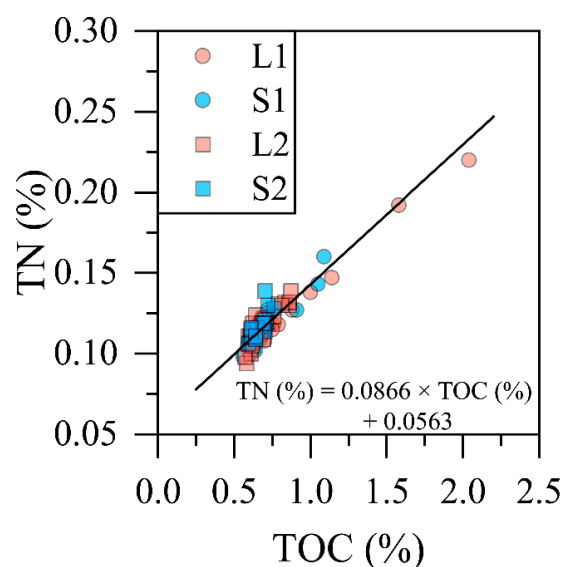
Figure 5. The plot of TOC versus TN for all subsamples along the sediment cores. Solid line is the geometric mean regression line for all subsamples.

Given that the δ^{13}C values for fresh *Spartina alterniflora* tissues were fairly enriched (ranging from -14.74‰ to -15.5‰; this study and [31]), the relatively more depleted δ^{13}C value of sedimentary organic carbon in both mangroves (ranging from -21.6‰ to -26.7‰) suggested a minor contribution from *Spartina alterniflora* to the local sedimentary organic carbon pool. This might be related to the geographic location of *Spartina alterniflora*, which was mostly distributed along the coastal fringes of the mangrove forest. The organic carbon from *Spartina alterniflora* was more easily transported by tides, hence the insufficient accumulation of materials. Although there are several watersheds, including the Ou River, around Yueqing Bay, a previous study suggested that seasonal river discharge accounts for a minor portion of the sediments delivered to the bay due to the small drainage areas and runoff, especially given that most sediments from the Ou River are deposited around the estuarine area next to the river's mouth [57]. Instead, the sediment materials from the Yangtze River and the inner shelf of the East China Sea, which were transported through the southerly Zhejiang–Fujian coastal current, were the dominant contributors to the sediments of the bay [57]. The measured δ^{13}C value for sedimentary organic carbon in the mudflat (S2) varied from -21.6‰ to -22.5‰, which was within the range of δ^{13}C values in the surface sediment of the inner shelf of the East China Sea obtained by Tan et al. ([58]; -20.8‰ to -22.9‰), Xing et al. ([59]; -20.1‰ to -22.7‰) and Wang et al. ([60]; -19.2‰ to -23.3‰).

4.3. Storage of Sedimentary Organic Carbon

In China's mangrove forest, 81.74% of the estimated carbon is stored in the top 1 m soil [61]. Compared to the top 1 m sedimentary organic carbon stock at different stations, station L1 stored the highest sedimentary organic carbon, followed by vegetation transition zone S1 (Figure 6). Stations L1 (81.93 Mg C_{org} ha^{-1}) and S1 (71.72 Mg C_{org} ha^{-1}) held higher carbon stock in the top meter than in the mudflat (station S2; 69.52 Mg C_{org} ha^{-1}), respectively, which is similar to the findings of previous studies conducted in other regions (e.g., in the Yinluo Bay, Guangdong ([62]); Shenzhen Bay, Guangdong ([63]) and Dongzhai Bay, Hainan ([28])). Furthermore, the carbon stock in the young mangrove forest was lower than in the mudflat, which was in accordance with expectation, because of the weaker capacity to capture carbon owing to the lower vegetation abundance. The offshore current could bring relatively more fine-grained sediments coupled with organic matter to the mudflat stand. Additionally, the top 40 cm carbon stock was the main reason for the highest carbon stock found in the interior of the old mangrove forest (station L1). The root system and history of mangrove colonisation could be the reasons for this. In contrast to the

mangrove plants in a tropical area whose developed root system might extend to 3–5 m, the root system of the mangrove forest has a limited distribution in the subtropical zone. This agrees with the observation that the amount of root debris drastically reduced in the sediment subsamples after 40–50 cm. Mangroves on Ximen Island were introduced in 1957 and have a development history of 64 years. The sedimentation rate in the mudflat was assumed to be 6.0 mm year^{-1} based on the average sedimentation rate in the inner shelf of the East China Sea reported by Liu et al. [64]. The sedimentation rate in the forest is often lower than that in the mudflat and marginal seas [15]. Hence, the top 40 cm depth could cover the history of mangroves on Ximen Island. As the mangroves age, the carbon stocks increase, as also supported by the evidence from a 66-year chrono-sequence in French Guiana's mangrove forests, according to which soil stocks increase as the forests age [65].
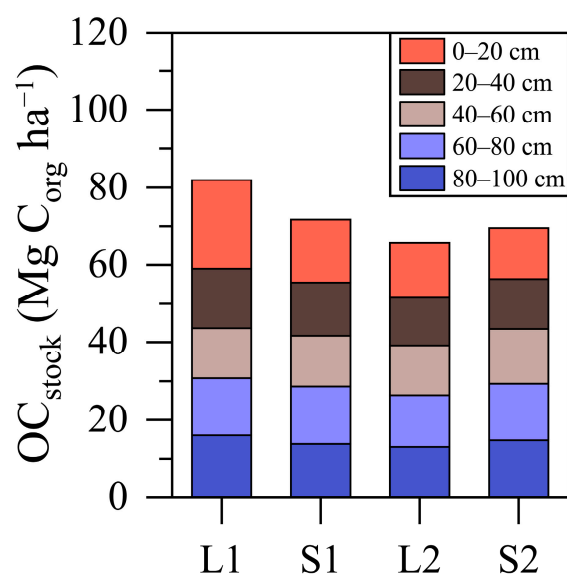

Figure 6. Variation in organic carbon stocks of each segment across distinct sampling stations along the whole 0–100 cm profile.

In our study, the sediment carbon sequestration in the old mangrove forest (81.9 Mg C_{org} ha^{-1}) was similar to the estimated soil organic carbon stocks in India (81.3 Mg C_{org} ha^{-1}) and New Zealand (73.5 Mg C_{org} ha^{-1}) but considerably lower than the estimated global mean value of 565.4 $\pm$ 25.7 Mg C_{org} ha^{-1} [66]. On Ximen Island, the mangrove community was composed of only one mangrove species. As reported, mixed mangroves had 20% higher soil carbon stocks than monotypic mangroves [23]. Additionally, climate plays a vital role in the size of mangrove carbon stocks. Mangroves in tropical areas usually have higher soil carbon storage than those in subtropical areas [23,67]. Moreover, the total mangrove area on Ximen Island was not large because of the limited planted area of the mangrove plants. As human activities (e.g., pond reconstruction) and the invasion of *Spartina alterniflora* become increasingly intensive, the mature mangrove forest becomes smaller. These observed patterns can explain the lower soil carbon sequestration in our study area. Accordingly, the development and implementation of management plans to protect and restore mangroves on Ximen Island need to consider the current declining trends in soil TOC storage and the expansion of saltmarshes into mangrove wetlands.

5. Conclusions

Our study evaluated both sediment accumulation and sedimentary organic carbon spatiotemporal patterns in mangroves characterized by different forest age and geomorphological settings. Fine-grained sediment deposition and accumulation were greater in older mangroves (~60 years) than in younger forests (~4 years) as a result of lower tidal flushing, especially in the inland low-energy sedimentation environment. Similarly, sedimentary

organic carbon derived from autochthonous sources was also higher in sites with older mangroves. This study showed that mangrove restoration and protection have a positive effect on the accumulation of fine-grained sediments and the increase in soil organic carbon stocks. These biogeochemical processes need to be considered when implementing mitigation plans to ameliorate the threat posed by sea-level rise and global warming.

Appendix A

Table A1. Results of Mz, σ, Sk, Ku and DBD.

Depth cm	Mz φ	σ φ	Sk	Ku	DBD $g\ cm^{-3}$
S1					
Surface	7.32	1.40	0.55	2.73	0.96
0–20	7.39 ± 0.06	1.43 ± 0.02	0.45 ± 0.07	2.67 ± 0.04	0.97 ± 0.03
20–40	7.37 ± 0.08	1.45 ± 0.03	0.46 ± 0.05	2.63 ± 0.06	1.01 ± 0.07
40–60	7.37 ± 0.07	1.44 ± 0.02	0.49 ± 0.06	2.65 ± 0.04	0.99 ± 0.04
60–80	7.38 ± 0.09	1.44 ± 0.01	0.46 ± 0.09	2.67 ± 0.06	1.19 ± 0.03
80–100	7.47 ± 0.02	1.44 ± 0.01	0.40 ± 0.01	2.59 ± 0.02	1.12 ± 0.07
L1					
Surface	7.51	1.39	0.41	2.74	0.84
0–20	7.53 ± 0.07	1.39 ± 0.00	0.45 ± 0.04	2.66 ± 0.05	0.93 ± 0.08
20–40	7.39 ± 0.08	1.44 ± 0.01	0.48 ± 0.08	2.67 ± 0.04	1.06 ± 0.11
40–60	7.44 ± 0.12	1.45 ± 0.02	0.44 ± 0.04	2.58 ± 0.04	0.99 ± 0.06
60–80	7.39 ± 0.11	1.45 ± 0.02	0.49 ± 0.07	2.61 ± 0.07	1.06 ± 0.04
80–100	7.45 ± 0.08	1.46 ± 0.04	0.44 ± 0.05	2.55 ± 0.02	1.18 ± 0.02
S2					
Surface	7.33	1.50	0.49	2.55	0.91
0–20	7.27 ± 0.10	1.41 ± 0.05	0.52 ± 0.13	2.87 ± 0.15	0.95 ± 0.06
20–40	7.35 ± 0.15	1.43 ± 0.08	0.49 ± 0.13	2.72 ± 0.24	1.00 ± 0.08
40–60	7.30 ± 0.20	1.48 ± 0.03	0.46 ± 0.18	2.74 ± 0.21	1.14 ± 0.03
60–80	7.30 ± 0.14	1.45 ± 0.03	0.50 ± 0.08	2.76 ± 0.14	1.13 ± 0.08
80−100	7.27 ± 0.13	1.44 ± 0.04	0.47 ± 0.11	2.74 ± 0.14	1.15 ± 0.05
L2					
Surface	7.12	1.35	0.49	3.00	0.82
0–20	7.27 ± 0.17	1.42 ± 0.05	0.43 ± 0.03	2.79 ± 0.22	0.83 ± 0.02
20–40	7.34 ± 0.13	1.44 ± 0.05	0.43 ± 0.08	2.70 ± 0.18	0.89 ± 0.04
40–60	7.34 ± 0.17	1.51 ± 0.03	0.41 ± 0.11	2.56 ± 0.10	1.08 ± 0.05
60–80	7.39 ± 0.10	1.48 ± 0.04	0.36 ± 0.13	2.65 ± 0.13	1.04 ± 0.06
80–100	7.33 ± 0.06	1.44 ± 0.04	0.54 ± 0.04	2.76 ± 0.11	0.97 ± 0.03

Table A2. Results of TOC, TN, C/N, δ^{13}C and OC$_{stock}$.

Depth cm	TOC %	TN %	C/N	δ^{13}C ‰	OC$_{stock}$ Mg C$_{org}$ ha^{-1}
S1					
Surface	0.91	0.127	8.3	−23.17	1.73
0–20	0.84 ± 0.21	0.126 ± 0.023	7.7 ± 0.65	−22.58 ± 0.37	16.23
20–40	0.68 ± 0.04	0.114 ± 0.007	7.0 ± 0.18	−22.48 ± 0.23	13.80
40–60	0.66 ± 0.03	0.113 ± 0.004	6.8 ± 0.14	−22.74 ± 0.12	13.02
60–80	0.62 ± 0.03	0.110 ± 0.003	6.6 ± 0.20	−22.76 ± 0.08	14.83
80–100	0.62 ± 0.04	0.105 ± 0.006	6.9 ± 0.31	−22.79 ± 0.10	13.84
L1					
Surface	2.04	0.220	10.8	−26.07	3.42
0–20	1.23 ± 0.49	0.157 ± 0.040	8.9 ± 1.17	−24.75 ± 1.01	22.88
20–40	0.73 ± 0.05	0.116 ± 0.002	7.4 ± 0.38	−23.29 ± 0.11	15.45
40–60	0.65 ± 0.02	0.116 ± 0.005	6.5 ± 0.07	−22.88 ± 0.15	12.85
60–80	0.69 ± 0.03	0.120 ± 0.006	6.8 ± 0.20	−22.85 ± 0.19	14.71
80–100	0.68 ± 0.02	0.112 ± 0.002	7.1 ± 0.30	−22.86 ± 0.24	16.04
S2					
Surface	0.70	0.139	5.9	−22.08	1.27
0–20	0.70 ± 0.05	0.125 ± 0.009	6.5 ± 0.43	−22.06 ± 0.27	13.21
20–40	0.64 ± 0.05	0.115 ± 0.005	6.5 ± 0.19	−22.33 ± 0.09	12.80
40–60	0.63 ± 0.02	0.110 ± 0.003	6.6 ± 0.10	−22.41 ± 0.12	14.19
60–80	0.64 ± 0.04	0.113 ± 0.003	6.6 ± 0.37	−22.57 ± 0.17	14.55
80–100	0.64 ± 0.03	0.114 ± 0.005	6.6 ± 0.33	−22.61 ± 0.13	14.77
L2					
Surface	0.79	0.131	7.1	−21.99	1.30
0–20	0.84 ± 0.03	0.132 ± 0.003	7.4 ± 0.24	−21.98 ± 0.24	13.94
20–40	0.70 ± 0.04	0.115 ± 0.006	7.1 ± 0.22	−22.30 ± 0.09	12.44
40–60	0.59 ± 0.02	0.100 ± 0.005	6.9 ± 0.27	−22.20 ± 0.14	12.75
60–80	0.64 ± 0.04	0.113 ± 0.006	6.6 ± 0.26	−22.34 ± 0.15	13.37
80–100	0.67 ± 0.04	0.121 ± 0.002	6.5 ± 0.37	−22.37 ± 0.14	13.03

References

1. Jennerjahn, T.C.; Ittekkot, V. Relevance of mangroves for the production and deposition of organic matter along tropical continental margins. *Naturwissenschaften* **2002**, *89*, 23–30. [CrossRef] [PubMed]
2. Duke, N.C. Mangrove Floristics and Biogeography Revisited: Further Deductions from Biodiversity Hot Spots, Ancestral Discontinuities, and Common Evolutionary Processes. In *Mangrove Ecosystems: A Global Biogeographic Perspective*; Springer International Publishing: Cham, Switzerland, 2017; pp. 17–53. ISBN 9783319622064.
3. Alongi, D.M. Carbon cycling and storage in mangrove forests. *Ann. Rev. Mar. Sci.* **2014**, *6*, 195–219. [CrossRef] [PubMed]
4. Cavanaugh, K.C.; Dangremond, E.M.; Doughty, C.L.; Park Williams, A.; Parker, J.D.; Hayes, M.A.; Rodriguez, W.; Feller, I.C. Climate-driven regime shifts in a mangrove–salt marsh ecotone over the past 250 years. *Proc. Natl. Acad. Sci. USA* **2019**, *116*, 21602–21608. [CrossRef] [PubMed]
5. Alongi, D.M. Carbon balance in salt marsh and mangrove ecosystems: A global synthesis. *J. Mar. Sci. Eng.* **2020**, *8*, 767. [CrossRef]
6. Alongi, D.M. Carbon sequestration in mangrove forests. *Carbon Manag.* **2012**, *3*, 313–322. [CrossRef]
7. Furukawa, K.; Wolanski, E. Sedimentation in Mangrove Forests. *Mangroves Salt Marshes* **1996**, *1*, 3–10. [CrossRef]
8. Furukawa, K.; Wolanski, E.; Mueller, H. Currents and Sediment Transport in Mangrove Forests. *Estuar. Coast. Shelf Sci.* **1997**, *44*, 301–310. [CrossRef]
9. Rovai, A.S.; Twilley, R.R.; Castañeda-Moya, E.; Riul, P.; Cifuentes-Jara, M.; Manrow-Villalobos, M.; Horta, P.A.; Simonassi, J.C.; Fonseca, A.L.; Pagliosa, P.R. Global controls on carbon storage in mangrove soils. *Nat. Clim. Chang.* **2018**, *8*, 534–538. [CrossRef]
10. Twilley, R.R.; Rovai, A.S.; Riul, P. Coastal morphology explains global blue carbon distributions. *Front. Ecol. Environ.* **2018**, *16*, 503–508. [CrossRef]
11. McKee, K.L.; Cahoon, D.R.; Feller, I.C. Caribbean mangroves adjust to rising sea level through biotic controls on change in soil elevation. *Glob. Ecol. Biogeogr.* **2007**, *16*, 545–556. [CrossRef]
12. Adame, M.F.; Kauffman, J.B.; Medina, I.; Gamboa, J.N.; Torres, O.; Caamal, J.P.; Reza, M.; Herrera-Silveira, J.A. Carbon Stocks of Tropical Coastal Wetlands within the Karstic Landscape of the Mexican Caribbean. *PLoS ONE* **2013**, *8*, e56569. [CrossRef]
13. Sasmito, S.D.; Sillanpää, M.; Hayes, M.A.; Bachri, S.; Saragi-Sasmito, M.F.; Sidik, F.; Hanggara, B.B.; Mofu, W.Y.; Rumbiak, V.I.; Hendri, S.T.; et al. Mangrove blue carbon stocks and dynamics are controlled by hydrogeomorphic settings and land-use change. *Glob. Chang. Biol.* **2020**, *26*, 3028–3039. [CrossRef] [PubMed]
14. Sasmito, S.D.; Kuzyakov, Y.; Lubis, A.A.; Murdiyarso, D.; Hutley, L.B.; Bachri, S.; Friess, D.A.; Martius, C.; Borchard, N. Organic carbon burial and sources in soils of coastal mudflat and mangrove ecosystems. *Catena* **2020**, *187*, 104414. [CrossRef]

15. Sanders, C.J.; Smoak, J.M.; Naidu, A.S.; Sanders, L.M.; Patchineelam, S.R. Organic carbon burial in a mangrove forest, margin and intertidal mud flat. *Estuar. Coast. Shelf Sci.* **2010**, *90*, 168–172. [CrossRef]

16. Meyers, P.A. Preservation of elemental and isotopic source identification of sedimentary organic matter. *Chem. Geol.* **1994**, *114*, 289–302. [CrossRef]

17. Bouillon, S.; Connolly, R.M.; Lee, S.Y. Organic matter exchange and cycling in mangrove ecosystems: Recent insights from stable isotope studies. *J. Sea Res.* **2008**, *59*, 44–58. [CrossRef]

18. Bouillon, S.; Dahdouh-Guebas, F.; Rao, A.V.V.S.; Koedam, N.; Dehairs, F. Sources of organic carbon in mangrove sediments: Variability and possible ecological implications. *Hydrobiologia* **2003**, *495*, 33–39. [CrossRef]

19. Tue, N.T.; Hamaoka, H.; Sogabe, A.; Quy, T.D.; Nhuan, M.T.; Omori, K. The application of δ13C and C/N ratios as indicators of organic carbon sources and paleoenvironmental change of the mangrove ecosystem from Ba Lat Estuary, Red River, Vietnam. *Environ. Earth Sci.* **2011**, *64*, 1475–1486. [CrossRef]

20. Kusumaningtyas, M.A.; Hutahaean, A.A.; Fischer, H.W.; Pérez-Mayo, M.; Ransby, D.; Jennerjahn, T.C. Variability in the organic carbon stocks, sources, and accumulation rates of Indonesian mangrove ecosystems. *Estuar. Coast. Shelf Sci.* **2019**, *218*, 310–323. [CrossRef]

21. Tue, N.T.; Ngoc, N.T.; Quy, T.D.; Hamaoka, H.; Nhuan, M.T.; Omori, K. A cross-system analysis of sedimentary organic carbon in the mangrove ecosystems of Xuan Thuy National Park, Vietnam. *J. Sea Res.* **2012**, *67*, 69–76. [CrossRef]

22. Stringer, C.E.; Trettin, C.C.; Zarnoch, S.J. Soil properties of mangroves in contrasting geomorphic settings within the Zambezi River Delta, Mozambique. *Wetl. Ecol. Manag.* **2016**, *24*, 139–152. [CrossRef]

23. Atwood, T.B.; Connolly, R.M.; Almahasheer, H.; Carnell, P.E.; Duarte, C.M.; Ewers Lewis, C.J.; Irigoien, X.; Kelleway, J.J.; Lavery, P.S.; Macreadie, P.I.; et al. Global patterns in mangrove soil carbon stocks and losses. *Nat. Clim. Chang.* **2017**, *7*, 523–528. [CrossRef]

24. Marchand, C. Soil carbon stocks and burial rates along a mangrove forest chronosequence (French Guiana). *For. Ecol. Manag.* **2017**, *384*, 92–99. [CrossRef]

25. Li, S.-B.; Chen, P.-H.; Huang, J.-S.; Hsueh, M.-L.; Hsieh, L.-Y.; Lee, C.-L.; Lin, H.-J. Factors regulating carbon sinks in mangrove ecosystems. *Glob. Chang. Biol.* **2018**, *24*, 4195–4210. [CrossRef] [PubMed]

26. Gao, Y.; Zhou, J.; Wang, L.; Guo, J.; Feng, J.; Wu, H.; Lin, G. Distribution patterns and controlling factors for the soil organic carbon in four mangrove forests of China. *Glob. Ecol. Conserv.* **2019**, *17*, e00575. [CrossRef]

27. Pham, V.H.; Luu, V.D.; Nguyen, T.T.; Koji, O. Will restored mangrove forests enhance sediment organic carbon and ecosystem carbon storage? *Reg. Stud. Mar. Sci.* **2017**, *14*, 43–52. [CrossRef]

28. Xiong, Y.; Liao, B.; Wang, F. Mangrove vegetation enhances soil carbon storage primarily through in situ inputs rather than increasing allochthonous sediments. *Mar. Pollut. Bull.* **2018**, *131*, 378–385. [CrossRef]

29. Tao, Y.; Huang, X.; Wang, X.; Zhong, Q.; Kang, Z. Spatial distribution of soil carbon and nitrogen stocks in Mangrove Wetland of Xiandao Park and Shajing in Guangxi. *Prog. Fish. Sci.* **2020**, *41*, 38–45, (In Chinese with English Abstract). [CrossRef]

30. Zhao, C.; Jiang, Z.; Wu, Y.; Liu, S.; Cui, L.; Zhang, J.; Huang, X. Origins of sediment organic matter and their contributions at three contrasting wetlands in a coastal semi-enclosed ecosystem. *Mar. Pollut. Bull.* **2019**, *139*, 32–39. [CrossRef]

31. Liao, Y.; Shou, L.; Tang, Y.; Zeng, J.; Chen, Q.; Yan, X. Effects of non-indigenous plants on food sources of intertidal macrobenthos in Yueqing Bay, China: Combining stable isotope and fatty acid analyses. *Estuar. Coast. Shelf Sci.* **2020**, *241*, 106801. [CrossRef]

32. Li, L.; Zhang, H.; Shi, A.; Li, D. Study on Wetland Landscape Pattern Change in the Ximen Island Marine Special Protected Area based on RS and GIS. *Remote Sens. Technol. Appl.* **2013**, *28*, 129–136.

33. Devaney, J.L.; Pullen, J.; Feller, I.C.; Parker, J.D. Low humidity and hypersalinity reduce cold tolerance in mangroves. *Estuar. Coast. Shelf Sci.* **2021**, *248*, 107015. [CrossRef]

34. Alexander, S.; Nelson, C.R.; Aronson, J.; Lamb, D.; Cliquet, A.; Erwin, K.L.; Finlayson, C.M.; de Groot, R.S.; Harris, J.A.; Higgs, E.S.; et al. Opportunities and Challenges for Ecological Restoration within REDD+. *Restor. Ecol.* **2011**, *19*, 683–689. [CrossRef]

35. Li, J.; Xu, H.; Ye, L.; Gu, J.; Wang, R. Introduction and afforestation technique of Kandelia candel to the north. *J. Zhejiang For. Sci. Technol.* **2001**, *21*, 51–53. (In Chinese)

36. Zheng, J.; Wang, J.; Chen, Q.; Xu, J.; Li, X.; Lu, X.; Lei, H.; Xia, H.; Zheng, S. Preliminary report on northward introduction experiment of several mangrove plants along the southern coast of Zhejiang Province. *J. Southwest For. Univ.* **2010**, *30*, 11–17, (In Chinese with English Abstract).

37. Chen, Q.; Yang, S.; Wang, J.; Liu, X.; Zheng, J.; Deng, R. The development of mangroves in Zhejiang Province. *J. Zhejiang Agric. Sci.* **2019**, *60*, 1177–1181, (In Chinese with English Abstract). [CrossRef]

38. Wang, A.; Chen, J.; Jing, C.; Ye, G.; Wu, J.; Huang, Z.; Zhou, C. Monitoring the invasion of Spartina alterniflora from 1993 to 2014 with Landsat TM and SPOT 6 satellite data in Yueqing Bay, China. *PLoS ONE* **2015**, *10*, e0135538. [CrossRef]

39. Zheng, R.; Ge, B.; Zhang, Y.; Zheng, X. The comparative study on the macrobenthic community ecology between the man-grove swamp and the naked tidal flat at the Yueqing Bay. *Ecol. Sci.* **2006**, *25*, 299–302, (In Chinese with English Abstract).

40. McManus, J. Grain size determination and interpretation. In *Techniques in Sedimentology*; Tucker, M., Ed.; Blackwell: Oxford, UK, 1988; pp. 63–85. ISBN 0-632-01361-3.

41. Blott, S.J.; Pye, K. GRADISTAT: A grain size distribution and statistics package for the analysis of unconsolidated sediments. *Earth Surf. Process. Landf.* **2001**, *26*, 1237–1248. [CrossRef]

42. Tu, Q.; Yang, S.; Zhou, Q.; Yang, J. Sediment transport and carbon sequestration characteristics along mangrove fringed coasts. *Acta Oceanol. Sin.* **2015**, *34*, 21–26. [CrossRef]

43. Van Santen, P.; Augustinus, P.G.E.F.; Janssen-Stelder, B.M.; Quartel, S.; Tri, N.H. Sedimentation in an estuarine mangrove system. *J. Asian Earth Sci.* **2007**, *29*, 566–575. [CrossRef]

44. Jiang, R.; Cheng, P.; Gao, J.; Wang, A. Impacts of mangrove on the dynamic process of bottom boundary layer. *Mar. Geol. Front.* **2020**, *36*, 37–44, (In Chinese with English Abstract). [CrossRef]

45. Mazda, Y.; Magi, M.; Kogo, M.; Hong, P.N. Mangroves as a coastal protection from waves in the Tong King delta, Vietnam. *Mangroves Salt Marshes* **1997**, *1*, 127–135. [CrossRef]

46. Zhu, Y.; Zhao, F.; Guo, J.; Wu, G.; Lin, G. Grain size characteristics of core sedimentation from the Gaoqiao mangrove area in Zhanjiang, Guangdong Province of southern China. *J. Beijing For. Univ.* **2017**, *39*, 9–17, (In Chinese with English Abstract). [CrossRef]

47. Sly, P.G.; Thomas, R.L.; Pelletier, B.R. Comparison of sediment energy-texture relationships in marine and lacustrine environments. *Hydrobiologia* **1982**, *91–92*, 71–84. [CrossRef]

48. Sihombing, Y.H.; Muskananfola, M.R.; A'in, C. Pengaruh kerapatan mangrove terhadap laju sedimentasi di desa bedono demak (The Effect of Mangrove Density on Sedimentation Rate in Bedono Village, Demak). *Manag. Aquat. Resour. J.* **2018**, *6*, 536–545. [CrossRef]

49. Gonneea, M.E.; Paytan, A.; Herrera-Silveira, J.A. Tracing organic matter sources and carbon burial in mangrove sediments over the past 160 years. *Estuar. Coast. Shelf Sci.* **2004**, *61*, 211–227. [CrossRef]

50. Lamb, A.L.; Wilson, G.P.; Leng, M.J. A review of coastal palaeoclimate and relative sea-level reconstructions using δ13C and C/N ratios in organic material. *Earth-Sci. Rev.* **2006**, *75*, 29–57. [CrossRef]

51. Khan, M.N.I.; Suwa, R.; Hagihara, A. Carbon and nitrogen pools in a mangrove stand of Kandelia obovata (S., L.) Yong: Vertical distribution in the soil-vegetation system. *Wetl. Ecol. Manag.* **2007**, *15*, 141–153. [CrossRef]

52. Zuo, X.; Cui, L.; Li, W.; Lei, Y.; Dou, Z.; Liu, Z.; Cai, Y.; Zhai, X. Spartina alterniflora leaf and soil eco-stoichiometry in the Yancheng coastal wetland. *Plants* **2021**, *10*, 13. [CrossRef] [PubMed]

53. Dittmar, T.; Lara, R.J. Molecular evidence for lignin degradation in sulfate-reducing mangrove sediments (Amazônia, Brazil). *Geochim. Cosmochim. Acta* **2001**, *65*, 1417–1428. [CrossRef]

54. Fourqurean, J.W.; Schrlau, J.E. Changes in nutrient content and stable isotope ratios of C and N during decomposition of seagrasses and mangrove leaves along a nutrient availability gradient in Florida Bay, USA. *Chem. Ecol.* **2003**, *19*, 373–390. [CrossRef]

55. Muzuka, A.N.N.; Shunula, J.P. Stable isotope compositions of organic carbon and nitrogen of two mangrove stands along the Tanzanian coastal zone. *Estuar. Coast. Shelf Sci.* **2006**, *66*, 447–458. [CrossRef]

56. Kennedy, H.; Gacia, E.; Kennedy, D.P.; Papadimitriou, S.; Duarte, C.M. Organic carbon sources to SE Asian coastal sediments. *Estuar. Coast. Shelf Sci.* **2004**, *60*, 59–68. [CrossRef]

57. Ji, X.; Zhang, Y.; Zhu, D. Study on Marine Environment and Recent Coastal Evolution of Yueqing Bay, Zhejiang Province, China. *Mar. Sci. Bull.* **2006**, *25*, 44–53, (In Chinese with English Abstract).

58. Tan, F.C.; Cai, D.L.; Edmond, J.M. Carbon isotope geochemistry of the Changjiang estuary. *Estuar. Coast. Shelf Sci.* **1991**, *32*, 395–403. [CrossRef]

59. Xing, L.; Zhang, H.; Yuan, Z.; Sun, Y.; Zhao, M. Terrestrial and marine biomarker estimates of organic matter sources and distributions in surface sediments from the East China Sea shelf. *Cont. Shelf Res.* **2011**, *31*, 1106–1115. [CrossRef]

60. Wang, Y.; Song, J.; Duan, L.; Yuan, H.; Li, X.; Li, N.; Zhang, Q.; Liu, J.; Ren, C. Combining sterols with stable carbon isotope as indicators for assessing the organic matter sources and primary productivity evolution in the coastal areas of the East China Sea. *Cont. Shelf Res.* **2021**, *223*, 104446. [CrossRef]

61. Liu, H.; Ren, H.; Hui, D.; Wang, W.; Liao, B.; Cao, Q. Carbon stocks and potential carbon storage in the mangrove forests of China. *J. Environ. Manag.* **2014**, *133*, 86–93. [CrossRef]

62. Wang, G.; Guan, D.; Peart, M.R.; Chen, Y.; Peng, Y. Ecosystem carbon stocks of mangrove forest in Yingluo Bay, Guangdong Province of South China. *For. Ecol. Manag.* **2013**, *310*, 539–546. [CrossRef]

63. Lunstrum, A.; Chen, L. Soil carbon stocks and accumulation in young mangrove forests. *Soil Biol. Biochem.* **2014**, *75*, 223–232. [CrossRef]

64. Liu, Y.C.; Hwang, C.; Han, J.; Kao, R.; Wu, C.R.; Shih, H.C.; Tangdamrongsub, N. Sediment-Mass accumulation rate and variability in the East China Sea detected by GRACE. *Remote Sens.* **2016**, *8*, 777. [CrossRef]

65. Walcker, R.; Gandois, L.; Proisy, C.; Corenblit, D.; Mougin, É.; Laplanche, C.; Ray, R.; Fromard, F. Control of "blue carbon" storage by mangrove ageing: Evidence from a 66-year chronosequence in French Guiana. *Glob. Chang. Biol.* **2018**, *24*, 2325–2338. [CrossRef] [PubMed]

66. Alongi, D.M. Global Significance of Mangrove Blue Carbon in Climate Change Mitigation. *Science* **2020**, *2*, 67. [CrossRef]

67. Sanders, C.J.; Maher, D.T.; Tait, D.R.; Williams, D.; Holloway, C.; Sippo, J.Z.; Santos, I.R. Are global mangrove carbon stocks driven by rainfall? *J. Geophys. Res. Biogeosci.* **2016**, *121*, 2600–2609. [CrossRef]